Modeling the Charging of Highly Oxidized Cyclohexene Ozonolysis Products Using Nitrate-Based Chemical Ionization

Journal:	*The Journal of Physical Chemistry*
Manuscript ID:	jp-2015-01818b.R1
Manuscript Type:	Article
Date Submitted by the Author:	n/a
Complete List of Authors:	Hyttinen, Noora; University of Helsinki, Chemistry Kupiainen-Määttä, Oona; University of Helsinki, Department of Physics Rissanen, Matti; University of Helsinki, Physics Muuronen, Mikko; University of Helsinki, Dep. of. Chem. Ehn, Mikael; University of Helsinki, Department of Physical Sciences, Kurtén, Theo; University of Helsinki, Chemistry

Modeling the Charging of Highly Oxidized Cyclohexene Ozonolysis Products Using Nitrate-Based Chemical Ionization

Noora Hyttinen,[†] Oona Kupiainen-Määttä,[‡] Matti P. Rissanen,[‡] Mikko Muuronen,[†] Mikael Ehn,[‡] Theo Kurtén[†,]*

[†]Department of Chemistry, University of Helsinki, P.O. BOX 55, FI-00014, Finland

[‡]Department of Physics, University of Helsinki, P.O. BOX 64, FI-00014, Finland

ABSTRACT. Several Extremely Low Volatility Organic Compounds (ELVOCs) formed in the ozonolysis of endocyclic alkenes have recently been detected in laboratory and field studies. These experiments have been carried out with Chemical Ionization Atmospheric Pressure interface Time-of-Flight mass spectrometers (CI-APi-TOF) with nitrate ions as reagent ions. The nitrate ion binds to the detected species through hydrogen bonds, but it also binds very strongly to one or two neutral nitric acid molecules. This makes the measurement highly selective when there is an excess amount of neutral nitric acid in the instrument. In this work we used quantum chemical methods to calculate the binding energies between a nitrate ion and several highly oxidized ozonolysis products of cyclohexene. These were then compared to the binding energies of nitrate ion – nitric acid clusters. Systematic configurational sampling of the molecules and clusters was carried out at the B3LYP/6-31+G* and ωB97xD/aug-cc-pVTZ levels, and the final

single point energies were calculated with DLPNO-CCSD(T)/def2-QZVPP. The binding energies were used in a kinetic simulation of the measurement system to determine the relative ratios of the detected signals. Our results indicate that at least two hydrogen bond donor functional groups (in this case, hydroperoxide, OOH) are needed for an ELVOC molecule to be detected in a nitrate ion CI-APi-TOF. Also, a double bond in the carbon backbone makes the nitrate cluster formation less favorable.

1 Introduction

Recently, much of the research on atmospheric new particle formation has focused on the effects of biogenic organic compounds on particle formation and growth rates.[1,2] Emissions of Biogenic Volatile Organic Compounds (BVOCs) have been estimated at 1150 Tg C/year globally.[3] In the atmosphere, these BVOCs may become oxidized to form less volatile compounds, which can contribute to organic aerosol production. The oxidation processes of BVOCs also affect air quality both locally and globally.[4,5]

Extremely Low Volatility Organic Compounds (ELVOCs[6]) are highly oxidized products of Volatile Organic Compounds (VOCs). These compounds generally have high O:C ratios, even reaching values exceeding unity. Recent studies have presented atmospheric observations of ELVOCs from the oxidation of biogenic monoterpenes with endocyclic double bonds, such as α-pinene and limonene.[7,8] According to Ehn et al.[7] and Rissanen et al.,[9] only a small portion of the oxidation processes lead to ELVOCs, with molar yields typically of the order of a few percent, even for the most efficiently ELVOC-forming alkenes. Nevertheless, ELVOCs are still likely to contribute very efficiently to particle formation and the growth of newly formed particles via

condensation,[10] and furthermore, ELVOCs have been demonstrated to have a significant effect on atmospheric organic aerosol loadings.

ELVOCs have been detected, for instance, using chemical ionization mass spectrometers (the chemical ionization atmospheric pressure interface time of flight mass spectrometer CI-APi-TOF[11] and the Cluster CIMS[12]). The detection with CI-APi-TOF is based on clustering with the nitrate ion (NO_3^-) through collisions with nitrate ions (Eq. 1), nitrate ion – nitric acid dimers (Eq. 2) and nitrate ion – nitric acid trimers (Eq. 3):

$$NO_3^- + (ELVOC) \rightleftharpoons (ELVOC)(NO_3^-) \quad (1)$$

$$HNO_3(NO_3^-) + (ELVOC) \rightleftharpoons HNO_3(NO_3^-)(ELVOC) \rightleftharpoons HNO_3 + (ELVOC)(NO_3^-) \quad (2)$$

$$(HNO_3)_2(NO_3^-) + (ELVOC) \rightleftharpoons (HNO_3)_2(NO_3^-)(ELVOC) \rightleftharpoons 2HNO_3 + (ELVOC)(NO_3^-) \quad (3)$$

Collisions of a bare nitrate ion with an ELVOC molecule lead directly to the formation of the (ELVOC)(NO_3^-) cluster. The evaporation lifetime of the cluster can be estimated from detailed balance, based on the collision rate and the equilibrium constant, which in turn can be calculated from the formation free energy of the cluster. In case of collisions with reagent ion dimers and trimers, on the other hand, the intermediate products of Equations 2 and 3 can lose either the ELVOC or the neutral nitric acid molecules, and the probability of forming the (ELVOC)(NO_3^-) cluster depends on the relative stabilities of this cluster and the $HNO_3(NO_3^-)$ dimer (Eq. 2) or $(HNO_3)_2(NO_3^-)$ trimer (Eq. 3). The binding energy between the neutral molecules and the reagent ions therefore determines which molecules can be observed with this instrument. The nitrate CI-APi-TOF technique has been shown to be sensitive towards highly-oxidized ELVOCs, but only a few species with lower oxygen content have been detected. Thus, it is possible that some ELVOCs, and especially their less oxidized precursors, remain undetected with this ionization method.

The reaction mechanisms that produce ELVOCs via autoxidation were recently investigated computationally and experimentally using cyclohexene.[9] The mechanism is in general agreement with previous studies on peroxy radical H-shifts and atmospheric autoxidation,[13-16] although the reaction chain proposed by Rissanen et al.[9] proceeds further than in many previously studied systems. The ELVOC formation mechanism from cyclohexene was suggested to proceed through a series of sequential unimolecular hydrogen shifts (H-shifts) of peroxy radicals, followed by O_2 additions to create a new peroxy radical with two more oxygen atoms. This enables a rapid increase in the O:C ratio of the reacting species. The radical reaction sequence is terminated by either a uni- or bimolecular reaction, leading to closed-shell ELVOC products.

Rissanen et al.[9] proposed the main unimolecular termination reaction in the ELVOC-forming mechanism from cyclohexene to be the loss of an OH radical following H-abstraction from a C-OOH carbon. This leads to products of the type $C_6H_8O_x$, where x is an odd number (5, 7, or 9). HO_2 loss following a 1,4 H-shift, and leading to the formation of a C=C double bond, was proposed by Rissanen et al.[9] as an explanation for the observed closed-shell products with an even number of oxygen atoms, e.g. $C_6H_8O_8$. Three main ELVOC products from cyclohexene, $C_6H_8O_7$, $C_6H_8O_8$ and $C_6H_8O_9$ were detected with the nitrate ion CI-APi-TOF by Rissanen et al.,[9] but no $C_6H_8O_5$ was detected even though high-level quantum chemical calculations predict its formation rate to be much faster than those of the detected products. A possible explanation for this is that the less oxidized $C_6H_8O_5$ products were not detected with the instrument due to weaker binding to the reagent ions. In order to clarify whether this is a valid assumption, or if the suggested formation pathway needs revision, we computed the binding energies for the ELVOC-type cyclohexene ozonolysis products with varying oxygen contents proposed by Rissanen et al.[9] and compared them to the binding energy of the nitric acid – nitrate ion cluster.

2 Methodology

The ELVOC molecules and their clusters have multiple conformers with exactly the same molecular structure, but with different geometrical orientations of the carbon backbone and functional groups, and thus different energies. The conformers with the lowest free energy are obtained through systematic conformer sampling as described in Rissanen et al.[9] The conformer distribution generation and initial geometry optimizations are done employing the Spartan '14 program.[17] The final geometry optimizations are performed for a reasonably small number (less than 50) of energetically best conformers using Gaussian 09[18] and the final single point energy calculations are computed with ORCA[19] version 3.0.1.

The free energies of formation are calculated for (ELVOC) molecules and (ELVOC)(NO_3^-) clusters where (ELVOC), in this work, is defined as one of the four highly oxidized ozonolysis products of cyclohexene: $C_6H_8O_5$, $C_6H_8O_7$, $C_6H_8O_8$ or $C_6H_8O_9$. Since measurements have not shown any significant abundances for any $(ELVOC)_2(NO_3^-)$ or $(ELVOC)(HNO_3)(NO_3^-)$ clusters[9] the free energy of formation is calculated only for $C_6H_8O_7(HNO_3)(NO_3^-)$ to confirm this result. The energies of $(ELVOC)_2(NO_3^-)$ structures were not studied further due to the practical demands of systematic conformer sampling for such large systems.

2.1 Conformer distribution and best conformers

All possible conformers are created with systematic conformational sampling using the MMFF force field. Initial single-point energies are calculated for all conformers with the density functional method B3LYP/6-31+G*. This approach was shown to be effective in predicting the relative energies of different conformers of the same chemical system.[9] At this point, all conformers more than 5 kcal/mol above the lowest energy conformer are discarded, and further

calculations are done with the smaller set of conformers thus obtained. Next, the geometries of the molecules and clusters are optimized using the same density functional and basis set. The conformers within 2 kcal/mol of the lowest energy are then further optimized using Gaussian 09 at the ωB97xD/aug-cc-pVTZ level. In this final optimization, the electronic energy differences relative to the conformer that had the lowest energy before the optimization always changed by less than 2 kcal/mol, indicating that the cut-off criterion is reasonable. Also in those cases where the lowest-energy conformer at the ωB97xD/aug-cc-pVTZ level was different from that at the B3LYP/6-31+G* level, the electronic energy of this new minimum was always within 0.5 kcal/mol of the energy of the best B3LYP conformer.

2.2 Single-point energy calculations

The final single-point energy calculation of the lowest energy conformer of each molecule and cluster is computed using ORCA with the DLPNO-CCSD(T)/def2-QZVPP method. The basis set was chosen after testing four different basis sets for $HNO_3(NO_3^-)$, $(HNO_3)_2(NO_3^-)$ and $C_6H_8O_5(NO_3^-)$ clusters (Supporting information).

Gibbs free energies of formation are obtained by adding the ωB97xD/aug-cc-pVTZ thermal corrections to the CCSD(T) electronic energies. The thermal corrections include the contributions from internal rotations calculated with the ωB97xD/aug-cc-pVTZ method using the HinderedRotor module of the Gaussian 09 program package.[20,21] The effect of hindered rotations on the Gibbs free energies was found to be relatively small, on the order of 1 kcal/mol, in agreement with test calculations using both one- and multidimensional hindered rotation corrections by Rissanen et al.[9]

2.3 Kinetic modeling

Once the formation energies have been calculated, chemical ionization of the ELVOCs in a measurement setup is simulated using the Atmospheric Cluster Dynamics Code (ACDC[22]). ACDC is a kinetic model that describes explicitly all collision and evaporation processes within a set of clusters, and numerically solves the time evolution of the cluster concentrations. Collision rates between ions and neutral molecules are computed based on the parameterization of Su and Chesnavich[23] using dipole moments and polarizabilities calculated by quantum chemistry. Evaporation rates are computed from the collision rates and the Gibbs free energies of formation using detailed balance. In addition, since $(ELVOC)_2(NO_3^-)$ or $(ELVOC)(HNO_3)(NO_3^-)$ were not detected in the cyclohexene ozonolysis measurements, we assume that these clusters break apart immediately upon being formed. As a test of this observation, only $C_6H_8O_7(HNO_3)(NO_3^-)$ is added to the simulation since its binding energy is calculated. The relative fragmentation probabilities (i.e. the yields of the different fragmentation pathways) of these and other larger clusters, whose formation free energies are not explicitly calculated, are derived from the relative formation free energies of the fragments (Eq.4), and added to the model.

$$p_i = \frac{e^{-\Delta G_i/RT}}{\sum_j e^{-\Delta G_j/RT}} \quad (4)$$

R is the gas constant, T is the temperature and ΔG_i is the Gibbs free energy of formation of cluster i. The relative fragmentation probabilities of $(HNO_3)_2(NO_3^-)(ELVOC)$ clusters are estimated by first assuming that one neutral nitric acid is evaporated, and then using the fragmentation probabilities of the $(HNO_3)(NO_3^-)(ELVOC)$ cluster, computed using Equation 4. The two fragmentation routes for $(HNO_3)(NO_3^-)(ELVOC)$ are HNO_3 + $(ELVOC)(NO_3^-)$ and $HNO_3(NO_3^-)$ + (ELVOC).

The simulation has two main parts (Fig. 1). In the first part the reagent ion distribution is created by producing nitrate ions at a constant rate and mixing them with HNO_3 molecules. The HNO_3 concentration will determine the reagent ion distribution that is then mixed with the sample in the second part of the simulation. Some HNO_3 molecules are also added to simulate the contaminant HNO_3 in the sample flow.

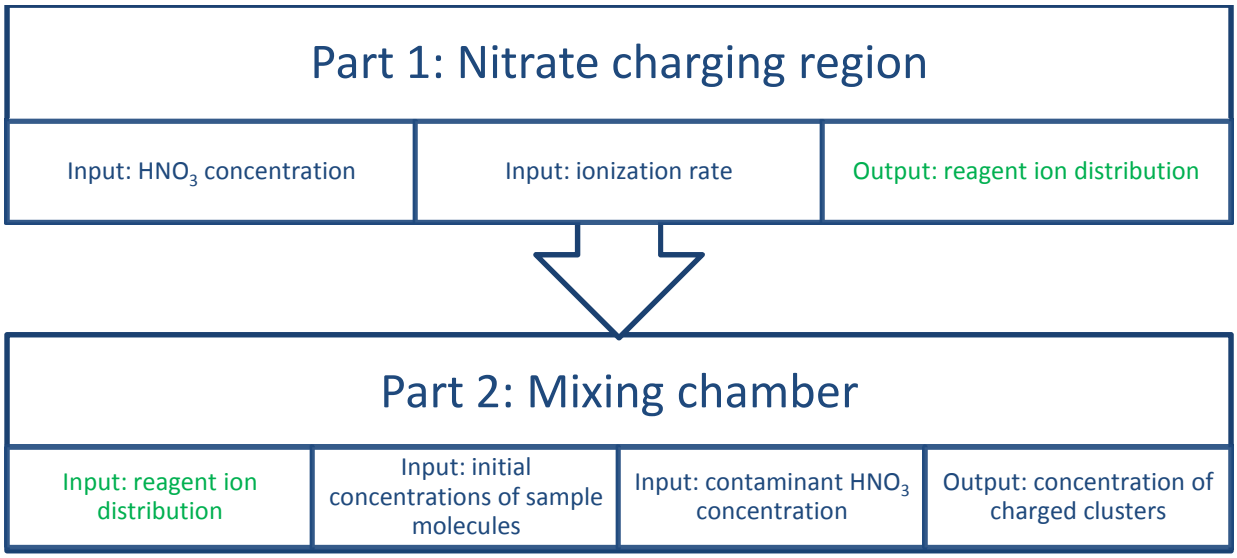

Figure 1. The parts of the chemical ionization simulation of the CI-APi-TOF.

In the simulation, the number of each ELVOC molecule introduced to the system is kept constant, as the purpose is not to estimate absolute concentrations, but the relative concentrations of different ELVOC species. The nitrate ion concentration is also kept constant at 10^7 cm^{-3}. The simulation creates a distribution of reagent ions by mixing HNO_3 and NO_3^- for 30 ms before the reagent ions come in contact with the ELVOCs. After this, the reagent ions and the ELVOCs have a 200 ms of mixing time, as in the typical application of the CI-APi-TOF instrument, during which some of the ELVOCs are charged by nitrate monomers (Eq. 1) or by taking a nitrate ion from a nitric acid dimer (Eq. 2) or trimer (Eq. 3).

In addition, an ELVOC molecule can collide with an (ELVOC)(NO_3^-) cluster (Eq. 5) in which case the ELVOC that has a weaker binding with the nitrate is more likely to evaporate from the cluster ($ELVOC^2$ in Eq. 5). These probabilities are also calculated with Equation 4.

$$(ELVOC^1) + (ELVOC^2)(NO_3^-) \rightleftharpoons (ELVOC^1)(ELVOC^2)(NO_3^-) \rightleftharpoons (ELVOC^2) + (ELVOC^1)(NO_3^-) \quad (5)$$

However, the reaction time in the CI-APi-TOF is kept short enough to avoid such secondary reactions, in order for the response of the instrument to be linear for all detected species. If ELVOC concentrations were to reach such high levels that reaction (5) became significant, measured instrumental calibration factors would no longer be applicable. Nevertheless, this reaction is included for completeness.

The simulation gives the ion counts of all molecules and clusters. By changing the HNO_3 concentration in the nitrate charging region and in the mixing chamber, we can see how the HNO_3 concentration in the measurements affects the charging of different ELVOCs (via the changes in the reagent ion distribution).

3 Results and Discussion

The free energies of the different conformers of the same molecules vary by several kcal/mol. The lowest free energy conformers of the four ELVOC molecules (Figs 2a-2d) and their nitrate clusters (Figs 2e-2h) at the ωB97xD/aug-cc-pVTZ level are presented in Figure 2. In the lowest energy conformers of the clusters the nitrate anion is bound to the ELVOC by one (Fig. 2e) or two (Figs 2f-2h) intermolecular hydrogen bonds with hydroperoxy groups. We also searched for conformers where all three hydroperoxy groups of $C_6H_8O_8$ and $C_6H_8O_9$ would take part in the intermolecular hydrogen bonding but the energetic cost (in formation free energy) for this was

found to be 2.3 and 3.5 kcal/mol compared to the conformers illustrated in Figures 2g and 2h respectively. This may be due to the additional angle strain of forming the third hydrogen bond.

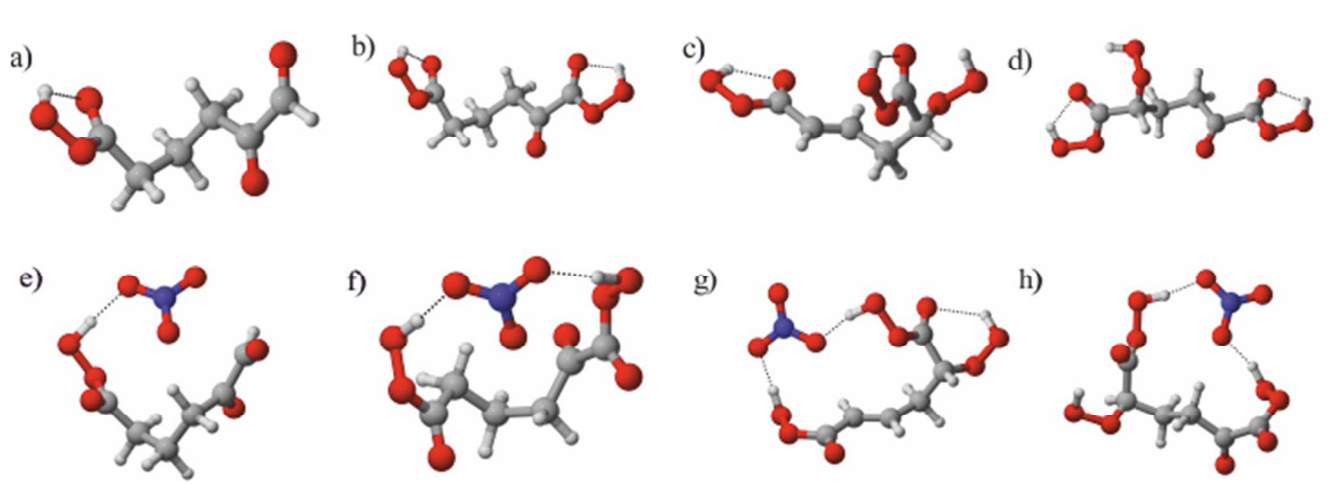

Figure 2. The optimized geometries of all ELVOC products and their nitrate clusters. From left to right a) $C_6H_8O_5$, b) $C_6H_8O_7$, c) $C_6H_8O_8$, d) $C_6H_8O_9$, e) $C_6H_8O_5(NO_3^-)$, f) $C_6H_8O_7(NO_3^-)$, g) $C_6H_8O_8(NO_3^-)$ and h) $C_6H_8O_9(NO_3^-)$.

3.1 Gibbs free energies of formation

The final Gibbs free energies of formation of the ELVOC-nitrate clusters relative to the formation free energy of the charged nitric acid dimer are presented in Table 1. The ELVOC cluster with the lowest free energy of formation is the $C_6H_8O_9(NO_3^-)$. In addition to $(ELVOC)(NO_3^-)$ clusters, the formation free energy of one $(ELVOC)(HNO_3)(NO_3^-)$ was also calculated to confirm that the larger clusters are not stable enough to be detected in the measurement setup. The formation free energy of $C_6H_8O_7(HNO_3)(NO_3^-)$ is 3 kcal/mol higher than the nitric acid trimer. $C_6H_8O_7$ and HNO_3 evaporate from a $C_6H_8O_7(HNO_3)(NO_3^-)$ cluster with an evaporation rate of 6.07×10^5 s^{-1} and 1.16×10^6 s^{-1} respectively. In comparison the evaporation rate of $C_6H_8O_7(NO_3^-)$ is only 4.88×10^{-5} s^{-1}. Also a HNO_3 colliding with a

$C_6H_8O_7(HNO_3)(NO_3^-)$ cluster will replace the $C_6H_8O_7$ molecule in the cluster with the probability of 99.4%. This might be the reason why $(ELVOC)(HNO_3)(NO_3^-)$ clusters are not detected in the measurements of cyclohexene products with the CI-APi-TOF.

Table 1. The Gibbs free energy of formation and the energies relative to nitric acid dimer (entries 1-5) or trimer (entries 6-7) at T = 298.15 K for a free neutral molecule forming a cluster with a charged cluster or an ion.

Entry	Nitrate cluster	$\Delta G(kcal/mol)$	$\Delta\Delta G(kcal/mol)$
	Two molecule clusters		
1	$HNO_3 + NO_3^- \rightarrow HNO_3(NO_3^-)$	-20.1	0.0
2	$C_6H_8O_5 + NO_3^- \rightarrow C_6H_8O_5(NO_3^-)$	-14.2	5.9
3	$C_6H_8O_7 + NO_3^- \rightarrow C_6H_8O_7(NO_3^-)$	-20.6	-0.5
4	$C_6H_8O_8 + NO_3^- \rightarrow C_6H_8O_8(NO_3^-)$	-18.8	1.3
5	$C_6H_8O_9 + NO_3^- \rightarrow C_6H_8O_9(NO_3^-)$	-24.4	-4.3
	Three molecule clusters		
6	$HNO_3 + HNO_3(NO_3^-) \rightarrow (HNO_3)_2(NO_3^-)$	-9.7	0.0
7	$C_6H_8O_7 + HNO_3(NO_3^-) \rightarrow C_6H_8O_7(HNO_3)(NO_3^-)$	-6.7	3.0

3.2 Determining initial concentrations of the cyclohexene ozonolysis products

The inlet of the CI-APi-TOF attempts to avoid mixing of the sheath flow containing nitric acid and reagent ions with the sample flow. In order to avoid mixing, the ions are electrostatically guided into the sample flow.[11] However, molecular diffusion will add HNO_3 also into the sample flow, as will any imperfect flow conditions leading to mixing of sample and sheath flows. In some experiments, especially during atmospheric sampling, the sample air itself may also contain non-negligible amounts of HNO_3. In other words, the exact HNO_3 concentration is hard

to estimate, and will likely not be constant over the 200 ms charging time. A reasonable estimate for a typical average value is on the order of 1-10 ppb, possibly even lower though unlikely to be much higher.

The simulation results in Figure 3 show how the HNO_3 concentration in the sample flow affects the charging efficiencies of the ELVOCs. With high contaminant HNO_3 concentrations the reagent ions are more likely to collide with HNO_3 than with ELVOC molecules. This gives lower (ELVOC)(NO_3^-) ion counts in high HNO_3 situations. Only the concentration of $C_6H_8O_9(NO_3^-)$ is almost unaffected by the HNO_3 concentration used in our simulations. All other (ELVOC)(NO_3^-) concentrations, as well as the concentration of the NO_3^- ion are significantly lower when high HNO_3 concentrations are present in the sample flow. With lower contaminant HNO_3 concentrations in the sample flow, the initial reagent ion distribution also has an effect on the concentrations, but when the contaminant HNO_3 concentration is high enough (> 1ppb), the initial reagent ion distribution no longer affects the charging of ELVOCs (Figs S1 and 3).

The signal of $C_6H_8O_5(NO_3^-)$ was not detected in the measurement of Rissanen et al.[9] According to the simulation, the sample could have contained a high concentration of $C_6H_8O_5$, but still would not have given a high enough $C_6H_8O_5(NO_3^-)$ concentration to be detected – provided that the contaminant HNO_3 concentration exceeded about 1 ppb (Fig. S1) or that the HNO_3 concentration in the nitrate charging region exceeds about 40 ppb, as it does in Figure 3.

The main difference between the measured ion signals and the relative concentrations in Figure 3 is that the concentration of free NO_3^- predicted by the simulations is much lower than observed. The only simulation conditions leading to high free NO_3^- concentrations are those where the HNO_3 concentration in both the nitrate charging region and in the sample flow are very low (Fig. S1). However, in these conditions the $C_6H_8O_5$ concentration would also be higher,

which does not agree with the measurements. A more probable explanation for the difference between the measured and the simulated NO_3^- signal may be non-thermal fragmentation processes occurring inside the mass spectrometer. Detailed investigation of these processes was beyond the scope of this study.

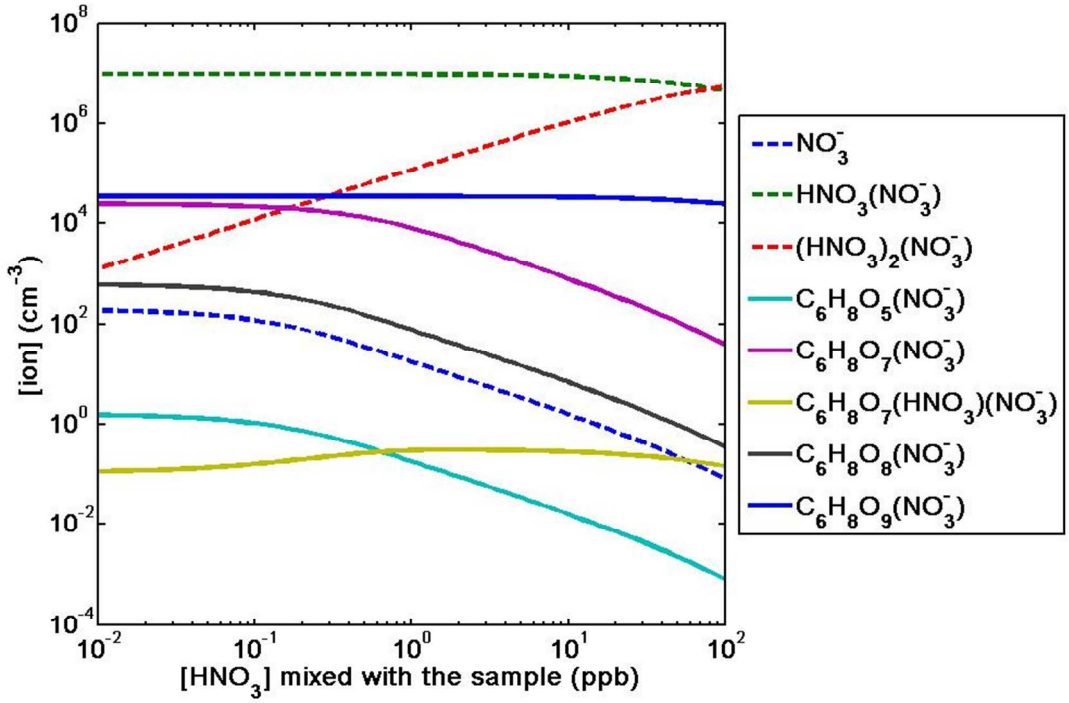

Figure 3. The ion concentrations of all charged clusters in the kinetic simulation, with a high (40 ppb) HNO_3 concentration in the nitrate charging region, as a function of the contaminant HNO_3 in the sample flow. The total ion concentration and all ELVOC concentrations are set to 10^7 cm^{-3} at the beginning of the chemical ionization simulation.

The measurements show that the ratios of the charged ELVOC cluster signals are $C_6H_8O_8/C_6H_8O_7 \approx 2$ and $C_6H_8O_9/C_6H_8O_7 \approx 9$ under typical experimental conditions. If the neutral nitric acid concentration was known and assuming that fragmentation of $(C_6H_8O_x)(NO_3^-)$ clusters (with x=7,8,9) in the mass spectrometer is minimal, this could be converted into a ratio of neutral ELVOC concentrations – assuming that the molecular structures used for the

calculations are correct and the modeling describes the charging process accurately. Unfortunately, the precise value of the experimental nitric acid concentration is not known. If the contaminant nitric acid concentration is very low, our calculations predict that the ratio of the concentrations of neutral $C_6H_8O_9$ and $C_6H_8O_7$ is close to the ratio of the ion signals, i.e. $[C_6H_8O_9]$ would then exceed $[C_6H_8O_7]$ by a factor of about nine. For higher contaminant nitric acid concentrations in the 1-10 ppb range, the predicted ratio of the $[C_6H_8O_9]$ and $[C_6H_8O_7]$ charging efficiencies is around 4-35 (Figure 4), implying that both species would have roughly equal concentrations. Due to the weaker binding of the proposed $C_6H_8O_8$ structure to nitrate, the neutral $C_6H_8O_8$ concentration would need to be at least 300 times higher than the $C_6H_8O_7$ concentration to obtain the observed ion cluster ratio of around two when 1-10 ppb of HNO_3 is mixed to the sample flow. The more likely explanation is that the $C_6H_8O_8$ molecules measured by Rissanen et al.[9] have a different structure than proposed in the same study.

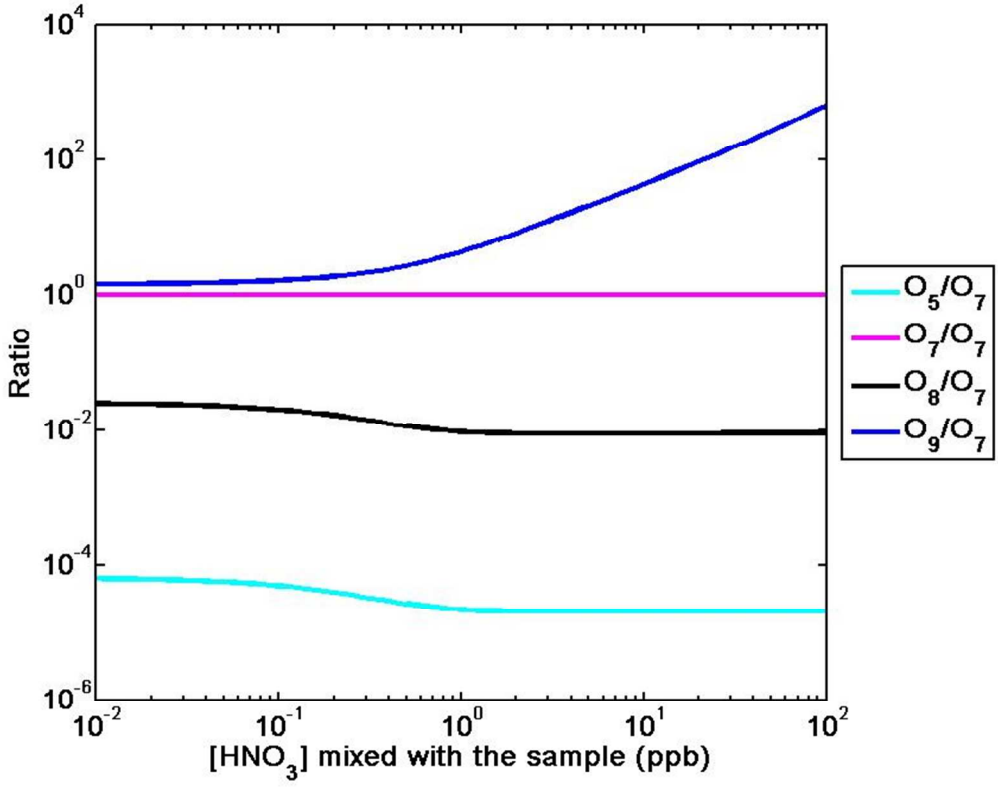

Figure 4. The ratios of each (ELVOC)(NO_3^-) and $C_6H_8O_7(NO_3^-)$ in the simulation of Figure 3. O_n denotes the nitrate cluster of an ELVOC that has n oxygen atoms.

4 Conclusions

The calculations strongly suggest that for a series of ELVOC structures proposed to be produced in ozonolysis initiated cyclohexene oxidation at atmospheric pressure, the addition of more OOH groups strengthens the binding of the molecule with NO_3^-. The exception is the suggested $C_6H_8O_8$ structure, which is found to be more weakly bound than the $C_6H_8O_7$ structure with one fewer OOH group. Presumably, the weaker binding of $C_6H_8O_8$ is related to the presence of a C=C double bond in the carbon chain. This creates ring strain when both ends of the molecule are bonded to the same nitrate ion. Also, additional oxygen atoms in the compound seem to strengthen the binding with nitrate ions even when the number of functional groups actually H-bonded to the nitrate ion remains the same.

The calculations explain why $C_6H_8O_5(NO_3^-)$ clusters were not detected by Rissanen et al.[9] Based on the kinetic simulations, $C_6H_8O_5(NO_3^-)$ is not seen in the measurements because its binding energy is much weaker than the binding energy of nitrate ion with a free nitric acid molecule. Also the fragmentation in the mass spectrometer may even further decrease the number of $C_6H_8O_5(NO_3^-)$ clusters that might be detected. Without considering fragmentation, the simulations show that even a very high initial neutral $C_6H_8O_5$ concentration does not lead to a measurable ion cluster signal, if either the contaminant nitric acid concentration in the instrument is higher than about one ppb, or that the nitric acid concentration in the nitrate charging region is higher than about 40 ppb.

Based on these calculations, ELVOCs need at least two OOH groups (or presumably other H-bond donating groups such as OH) to have a more energetically favorable cluster structure than charged nitric acid dimers or trimers. This means that the less oxidized oxidation products of cyclohexene and other alkenes can probably not be detected with a CI-APi-TOF using nitrate reagent ions. In the future, additional calculations could be made for compounds with different functional groups to see if, for instance, also OH groups bond to NO_3^- as strongly as OOH groups. Calculations with more sensitive (less selective) reagent ions such as iodine are also underway.

The formation of the $C_6H_8O_8$ molecule studied here is unlikely to be significantly faster than the formation of $C_6H_8O_7$ and $C_6H_8O_9$ during cyclohexene ozonolysis,[9] as the formation of $C_6H_8O_8$ requires a sterically strained 1,4 H-shift. Based on the clustering free energy computed here, it therefore seems unlikely that enough $C_6H_8O_8$ could be formed via this channel to explain the relatively high ion cluster signal of $C_6H_8O_8(NO_3^-)$. Thus, we tentatively conclude that the observed signal for $C_6H_8O_8$ probably corresponds to a different structure with the same chemical formula, which has a higher formation rate, a stronger binding with nitrate, or both. For example, bimolecular reactions of the intermediate peroxy radicals via an alkoxy channel could lead to a $C_6H_8O_8$ product with both OH and OOH groups,[24] which would presumably bind more strongly to a nitrate ion.

The simulations indicate that the relative ion cluster signals obtained in a CI-APi-TOF measurement setup strongly depend on the nitric acid concentration in the instrument. With a higher nitric acid concentration, more nitrate ions will be bound to nitrate ion – nitric acid dimers and trimers that are typically less efficient in charging the ELVOCs than the plain nitrate ion. The $(ELVOC)(NO_3^-)$ cluster that has the strongest binding energy is detected with a highest

intensity when more HNO_3 is added to the instrument. Determining the initial concentrations of more weakly binding molecules in the sample is in general not possible without knowledge of the HNO_3 concentration in the instrument, and the fragmentation processes in the mass spectrometer. However, if the nitric acid concentrations and the fragmentation probabilities were known, then quantum chemical data could be used to obtain estimates of the relative ratios of neutral molecules from the measured ion signals. Measurements with varying concentrations of added nitric acid, or with an isotopically labeled nitric acid tracer allowing the determination of the exact concentration of nitric acid, in conjunction with quantum chemical calculations such as those presented here, could thus help determine the concentration or yield ratios of different ELVOCs formed in atmospheric autoxidation.

ASSOCIATED CONTENT

Supporting Information

Tables S1-S4: Table S1 Comparison of different basis sets for DLPNO-CCSD(T) calculations, Table S2 Comparison of ωB97xD and CCSD(T) electronic energies, Table S3 Absolute final point electronic energies and corrections for all molecules and clusters, Table S4 Collision and evaporation rates. **Section S1** Cartesian coordinates of the lowest-energy structures. **Figure S1** Simulation of the measurement system with a lower nitric acid concentration in the nitrate charging region. This material is available free of charge via the Internet at http://pubs.acs.org

AUTHOR INFORMATION

Corresponding Author

*E-mail: theo.kurten@helsinki.fi. Phone: +358 50 526 0123.

ACKNOWLEDGMENT

We thank the Academy of Finland for funding. We thank CSC-IT Center for Science in Espoo, Finland, for computing time.

REFERENCES

(1) Kulmala, M.; Kontkanen, J.; Junninen, H.; Lehtipalo, K.; Manninen, H. E.; Nieminen, T.; Petäjä, T.; Sipilä, M.; Schobesberger, S.; Rantala, P.; et al. Direct Observations of Atmospheric Aerosol Nucleation. *Science* **2013,** *339*, 943-946.

(2) Donahue, N. M.; Ortega, I. K.; Chuang, W.; Riipinen, I.; Riccobono, F.; Schobesberger, S.; Dommen, J.; Baltensperger, U.; Kulmala, M.; Worsnop, D. R.; et al. How Do Organic Vapors Contribute to New-Particle Formation? *Faraday Discuss.* **2013,** *165*, 91-104.

(3) Guenther, A.; Hewitt, N.; Erickson, D.; Fall, R.; Geron, C.; Graedel, T.; Harley, P.; Klinger, L.; Lerdau, M.; McKay, W. A.; et al. A Global Model of Natural Volatile Organic Compound Emissions. *J. Geophys. Res., [Atmos.]* **1995,** *100*, 8873-8892.

(4) Kim, S.; Karl, T.; Guenther, A.; Tyndall, G.; Orlando, J.; Harley, P.; Rasmussen, R.; Apel, E. Emissions and Ambient Distributions of Biogenic Volatile Organic Compounds (BVOC) in a Ponderosa Pine Ecosystem: Interpretation of PTR-MS Mass Spectra. *Atmos. Chem. Phys.* **2010,** *10*, 1759-1771.

(5) McFiggans, G. Involatile Particles from Rapid Oxidation. *Nature* **2014,** *506*, 442-443.

(6) Donahue, N. M.; Kroll, J. H.; Pandis, S. N.; Robinson, A. L. A Two-Dimensional Volatility Basis Set. Part 2: Diagnostics of Organic-Aerosol Evolution. *Atmos. Chem. Phys.* **2012,** *12*, 615-634.

(7) Ehn, M.; Thornton, J. A.; Kleist, E.; Sipilä, M.; Junninen, H.; Pullinen, I.; Springer, M.; Rubach, F.; Tillmann, R.; Lee, B.; et al. A Large Source of Low-Volatility Secondary Organic Aerosols. *Nature* **2014,** *506*, 476-479.

(8) Jokinen, T.; Sipilä, M.; Richters, S.; Kerminen, V.-M.; Paasonen, P.; Stratmann, F.; Worsnop, D.; Kulmala, M.; Ehn, M.; Herrmann, H.; et al. Rapid Autoxidation Forms Highly Oxidized RO_2 Radicals in the Atmosphere. *Angew. Chem., Int. Ed.* **2014,** *53*, 14596-14600.

(9) Rissanen, M. P.; Kurtén, T.; Sipilä, M.; Thornton, J. A.; Kangasluoma, J.; Sarnela, N.; Junninen, H.; Jørgensen, S.; Schallhart, S.; Kajos, M. K.; et al. The Formation of Highly Oxidized Multifunctional Products in the Ozonolysis of Cyclohexene. *J. Am. Chem. Soc.* **2014,** *136*, 15596-15606.

(10) Riipinen, I.; Pierce, J. R.; Yli-Juuti, T.; Nieminen, T.; Häkkinen, S.; Ehn, M.; Junninen, H.; Lehtipalo, K., Petäjä, T.; Slowik, J.; et al. Organic Condensation: a Vital Link Connecting Aerosol Formation to Cloud Condensation Nuclei (CCN) Concentrations. *Atmos. Phys. Chem.* **2011,** *11*, 3865-3878.

(11) Jokinen, T.; Sipilä, M.; Junninen, H.; Ehn, M.; Lönn, G.; Hakala, J.; Petäjä, T.; Mauldin III, R. L.; Kulmala, M.; Worsnop, D. R. Atmospheric Sulphuric Acid and Neutral Cluster Measurements Using CI-APi-TOF. *Atmos. Chem. Phys.* **2012,** *12*, 4117-4125.

(12) Zhao, J.; Eisele, F. L.; Titcombe, M.; Kuang, C.; McMurry, P. H. Chemical Ionization Mass Spectrometric Measuremens of Atmospheric Neutral Clusters Using the Cluster-CIMS. *J. Geophys. Res., [Atmos.]* **2010,** *115,* D08205.

(13) Crounse, J. D.; Knap, H. C.; Ørnsø, K. B.; Jørgensen, S.; Paulot, F.; Kjaergaard, H. G.; Wennberg, P. O. Atmospheric Fate of Methacrolein. 1. Peroxy Radical Isomerization Following Addition of OH and O_2. *J. Phys. Chem. A* **2012,** *116*, 5756-5762.

(14) Crounse, J. D.; Nielsen, L. B.; Jørgensen, S.; Kjaergaard, H. G.; Wennberg, P. O. Autoxidation of Organic Compounds in the Atmosphere. *J. Phys. Chem. Lett.* **2013,** *4*, 3513-3520.

(15) Vereecken, L.; Francisco, J. S., Theoretical Studies of Atmospheric Reaction Mechanisms in the Troposphere. *Chem. Soc. Rev.* **2012,** *41*, 6259-6293.

(16) Vereecken, L.; Nguyen, T. L.; Hermans, I.; Peeters, J. Computational Study of the Stability of a-Hydroperoxyl- or a-alkylperoxyl Substituted Alkyl Radicals. *Chem. Phys. Lett.* **2004,** *393*, 432-436.

(17) *Spartan '14;* Wavefunction Inc.: Irvine CA, 2014.

(18) Frisch, M. J.; Trucks, G. W.; Schlegel, H. B.; Scuseria, G. E.; Robb, M. A.; Cheeseman, J. R.; Scalmani, G.; Barone, V.; Mennucci, B.; Petersson, G. A.; et al. *Gaussian 09,* Revision C.01 and D.01; Gaussian Inc.: Wallingford CT, 2009.

(19) Neese, F. The ORCA Program System. *Wiley Interdiscip. Rev. Comput. Mol. Sci.* **2012,** *2*, 73-78.

(20) Ayala, P. Y.; Schlegel, H. B. Identification and Treatment of Internal Rotation in Normal Mode Vibrational Analysis. *J. Chem. Phys.* **1998,** *108*, 2314-2325.

(21) McClurg, R. B.; Flagan, R. C.; Goddard III, W. A. The Hindered Rotor Density-of-States Interpolation Function. *J. Chem. Phys.* **1997,** *106*, 6675-6680.

(22) Kupiainen-Määttä, O.; Olenius, T.; Kurtén, T.; Vehkamäki, H. CIMS Sulfuric Acid Detection Efficiency Enhanced by Amines Due to Higher Dipole Moments: A Computational Study. *J. Phys. Chem. A* **2013,** *117*, 14109-14119.

(23) Su, T.; Chesnavich, W. J. Parametrization of the Ion-Polar Molecule Collision Rate Constant by Trajectory Calculations. *J. Chem. Phys.* **1982,** *76*, 5183-5185.

(24) Mentel, T. F.; Springer, M.; Ehn, M.; Kleist, E.; Pullinen, I.; Kurtén, T.; Rissanen, M.; Wahner, A.; Wildt, J. Formation of Highly Oxidized Multifunctional Compounds: Autoxidation of Peroxy Radicals Formed in the Ozonolysis of Alkenes – Deduced from Structure-Product Relationships. *Atmos. Chem. Phys. Discuss.* **2015,** *15*, 2791-2851.

Table of Contents graphic

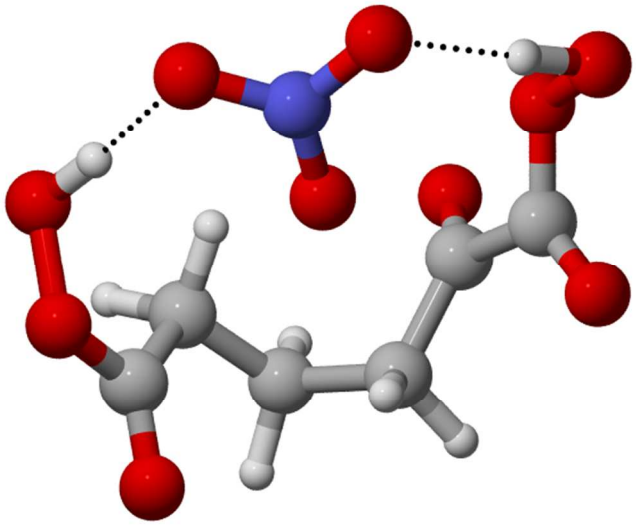

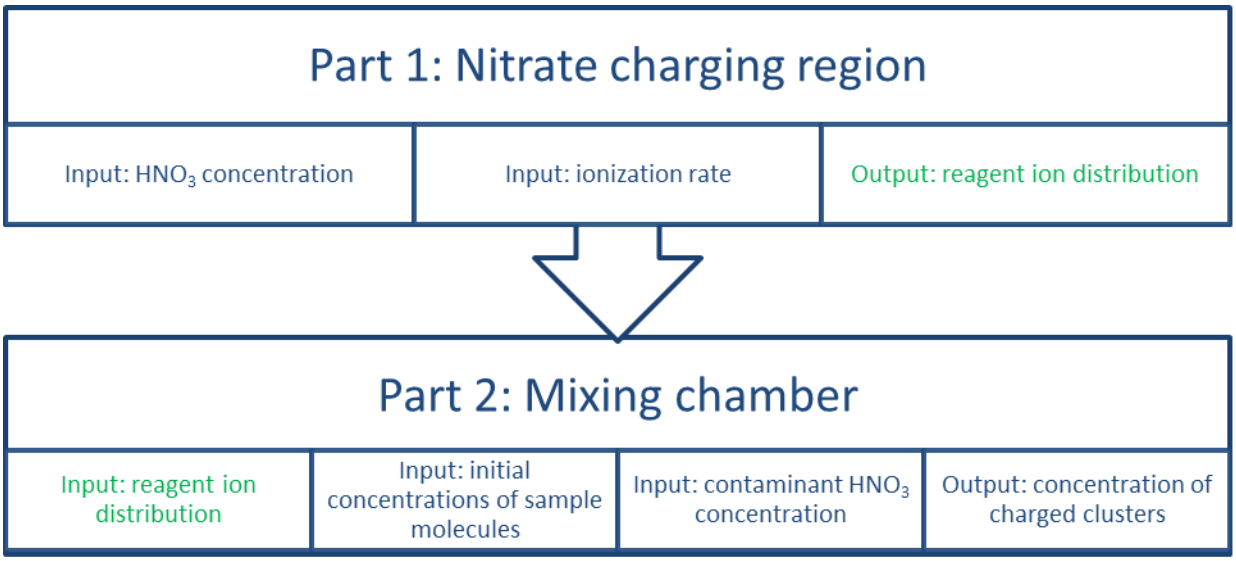
Part 1: Nitrate charging region
Input: HNO_3 concentration
Input: ionization rate
Output: reagent ion distribution
Part 2: Mixing chamber
Input: reagent ion distribution
Input: initial concentrations of sample molecules
Input: contaminant HNO_3 concentration
Output: concentration of charged clusters

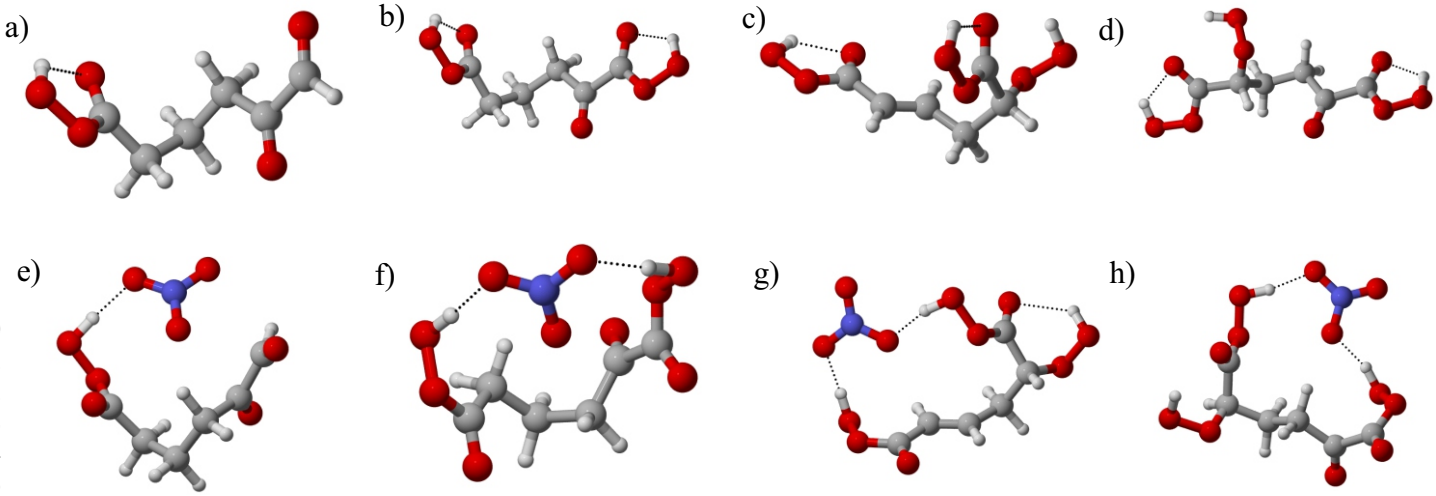
a)
b)
c)
d)
e)
f)
g)
h)